Engineering Structures 212 (2020) 110505

Contents lists available at ScienceDirect

Engineering Structures

journal homepage: www.elsevier.com/locate/engstruct

A hybrid methodology using finite elements and neural networks for the analysis of adhesive anchors exposed to hurricanes and adverse environments

Sálvio Aragão Almeida Jr., Serhan Guner*

Department of Civil and Environmental Engineering, University of Toledo, Toledo, OH 43607, USA

ARTICLE INFO

Keywords:
Anchorage
Concrete
Cracking
Failure
Finite elements
Hurricanes
Artificial neural networks
Nonlinear analysis
Pullout
Simulation

ABSTRACT

Hurricanes are responsible for approximately $28bn of damage every year in the United States alone, which may reach $151bn by 2075 due to the intensification of climate change according to certain prediction models. Approximately 35% of this damage is estimated to come from anchorage failures of non-structural components (NSCs). Severe exposure of NSCs to the adverse environments (such as elevated temperatures and long-term concrete cracking) and wind-induced bending effects during hurricanes promote anchorage failures. Three-dimensional (3D) nonlinear finite element (NLFE) analysis methods are currently required for simulating the anchor behavior due to the 3D phenomena involved; however, these models are rather complex and computationally prohibitive for analyzing large systems commonly encountered in practice. This study proposes a 2D analysis methodology that combines the strengths of 3D numerical modeling with the artificial neural network techniques to rapidly simulate the anchorage behavior while accounting for the effects of the adverse environmental exposure, concrete cone failure, and wind-induced bending effects. The methodology, which is validated with experimental data and 3D NLFE analyses, employs three distinct techniques as follows: (*i*) a novel modeling approach, 'the Equivalent Cone Method,' to accurately simulate the concrete cone breakout failure, (*ii*) analytical equations developed to account for wind-induced beam bending and elevated temperatures, and (*iii*) a multilayered feed-forward artificial neural network, trained and tested with the experimental data from a worldwide database, to rapidly account for long-term concrete cracking experienced by rooftop slabs. By employing these techniques, the proposed methodology permits the use of 2D NLFE models for anchor analysis with accuracies comparable to advanced 3D NLFE models but at a fraction of the computational cost.

1. Introduction

Since 1980, the United States has lost $935bn to tropical storm damage [1]. Recent studies suggest that this damage is rapidly increasing due to urbanization of the coastal areas and climate change [2–9]. The unusually active hurricane seasons of 2017 and 2018 in the Atlantic demonstrate this trend. More recently in 2019, a so-called 'bomb cyclone' brought hurricane-like wind speeds farther into the U.S. continental land, including the Midwest, affecting areas that are neither accustomed nor prepared to withstand strong winds. If this trend continues, the current post-storm cost of $28bn/year (as of the year 2015) may reach $151bn/year by 2075 [3].

Approximately 35% of hurricane loss is estimated to come from damage to non-structural components (NSCs) [10], such as heating, ventilation, and air-conditioning (HVAC) systems; solar panels; inverters; and renewable energy systems (see Fig. 1). This number is expected to increase as the next-generation zero-energy buildings will contain a significantly higher number of NSCs anchored to their rooftops.

Reconnaissance studies by the (FEMA) indicate that the main cause of hurricane damage to is poor anchorage [14]. NSCs are typically anchored to the rooftops of buildings through post-installed anchors and expected to provide service for several decades. Adhesive anchors are commonly used since they provide the flexibility to adjust the installation location while providing high load capacities. However, they are sensitive to adverse environmental conditions commonly encountered at rooftop levels, which weaken them over several decades and make them vulnerable to strong windstorms.

An important environmental condition is the elevated temperatures present on the roof, which can exceed 75 °C in the U.S. even in areas

* Corresponding author.
E-mail addresses: saragao@rockets.utoledo.edu (S. Aragão Almeida), serhan.guner@utoledo.edu (S. Guner).

https://doi.org/10.1016/j.engstruct.2020.110505
Received 10 October 2019; Received in revised form 1 March 2020; Accepted 9 March 2020
Available online 19 March 2020

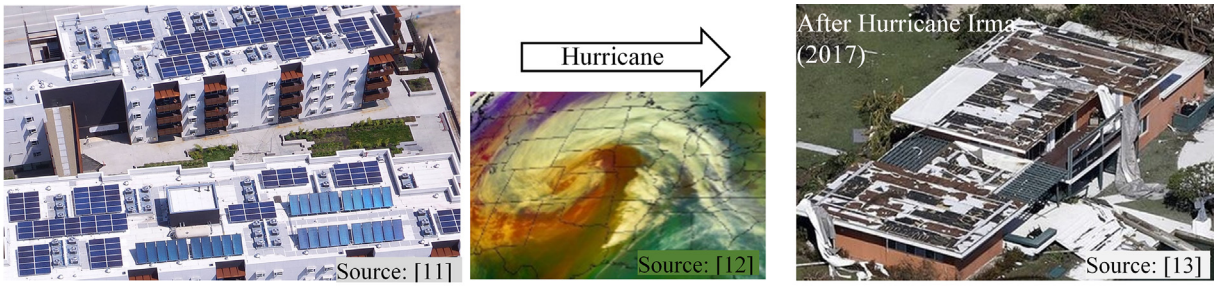

Fig. 1. Impacts of hurricanes on the next-generation zero-energy buildings [11,12,13].

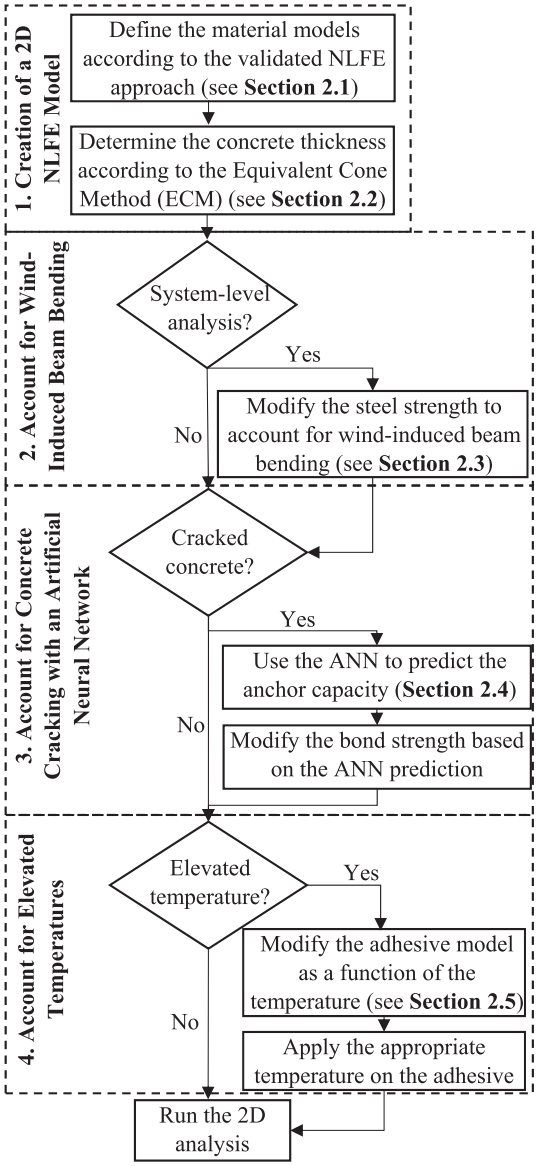

Fig. 2. Stages of the proposed methodology.

considered cold, such as the Midwest [15]. These high temperatures soften the resin used in adhesive anchors, affecting their hurricane performance [e.g. 16]. Another adverse condition is the presence of concrete cracks and deterioration in the rooftop slabs where NSCs are anchored. Concrete members routinely develop cracks over time due to the application of daily service loads. Research shows that the anchors act as a 'crack magnet,' attracting cracks to form and propagate around themselves [17]. However, in most current numerical analysis techniques, there is a lack of material models to account for the bond damage and reduced adhesive performance when it is in contact with cracked concrete [17], which may lead to unsafe designs and premature anchor failures during windstorms.

Aggravating this scenario, most current analysis methods and design provisions [e.g. 18, 19] are based on the isolated performance of single anchors, which neglects the system-level phenomena such as wind-induced bending of the supporting beams, which causes additional stresses during windstorms. Due to the lack of simple analysis methods, these effects are not typically considered in anchor design, which may lead to premature anchor failures during windstorms.

To study and advance the current knowledge on how these adverse effects impact the anchorage performance, 3D nonlinear finite element (NLFE) analyses are an appropriate option since they can simulate the 3D phenomena involved. However, from a computational and practical point of view, 3D NLFE models are rather complex and computationally expensive (i.e. typically requiring hours). 2D NLFE models, on the other hand, are much simpler to create and run, and take significantly less time to complete (i.e., typically minutes). However, there is a current challenge regarding the consideration of the 3D phenomena in these models, such as the wind-induced bending, and the conical concrete stresses, cracking and failure modes.

This paper presents a novel methodology to permit the use of 2D NLFE models in the analysis of anchors that accounts for effects of the adverse rooftop environment and wind-induced bending while achieving an accuracy similar to 3D NLFE models. To create this methodology, 3D high-fidelity nonlinear NLFE models are created, validated (with the data from 14 experimental tests), and employed to generate the data from single-anchor and NSC-anchorage system analyses. The data generated is employed to (*i*) create and validate a 2D modeling approach (Equivalent Cone Method or ECM) which permits 2D models to accurately predict the anchor load capacity in concrete breakout failure mode – a 3D phenomenon, (*ii*) derive analytical equations to quantify and account for the effects of wind-induced beam bending and elevated temperatures in 2D models, and (*iii*) develop, train, and test an artificial neural network (ANN) with 160 experimental results to account for concrete cracking in anchor analysis in a much simpler manner than currently possible. By taking advantage of these new techniques, the proposed methodology can predict the anchor response, requiring much less time and effort while still providing an accuracy comparable to the 3D NLFE models.

2. Overview of the 2D anchorage analysis methodology

An overview of the proposed 2D analysis methodology is presented in Fig. 2. The first stage of the methodology requires the creation of a 2D NLFE model. To accurately predict the stiffness and load capacity of an anchor, the NLFE model considers the nonlinear stress-strain relationship in the concrete, steel and adhesive, and the interactions between these components, as discussed in Section 2.1. To accurately

predict the concrete breakout capacity using 2D models, the Equivalent Cone Method (ECM) is developed in Section 2.2.

The second stage of the methodology, which is needed for the system-level analysis, accounts for the wind-induced bending of NSC-supporting beams. Strong wind loads can bend supporting beams in the direction perpendicular to the wind, which in turn bends the anchors, reducing their load capacities. To consider this effect, the yielding and ultimate strengths of the anchor rods are reduced according to the analytical equations derived in Section 2.3 from the results of the system-level investigations.

The third stage of the methodology accounts for the long-term concrete cracking which may be present in the rooftop slab where the NSC is installed. To consider this effect, an artificial neural network (ANN) model is developed in Section 2.4. This network predicts the anchor capacity in cracked concrete and uses this value to calculate a reduced bond strength for use in the 2D NLFE model.

The fourth stage of the methodology accounts for the effects of elevated temperatures. If the adhesive anchors are exposed to elevated temperatures above 40 °C, the resin around the anchor may soften, resulting in a reduction of the bond strength and stiffness. This phenomenon is considered by modifying the bond properties for use in the 2D model according to the new analytical equations developed in Section 2.5. If both concrete cracking and elevated temperatures are present simultaneously, the ANN model is used first, followed by the analytical equations.

2.1. Definition and validation of the material models

The 2D NLFE model requires defining the nonlinear relationships between stresses and strains in the concrete, steel, and adhesive. For this purpose, a set of advanced material models is validated with the results from the 3D high-fidelity NLFE models and experimental data as discussed in this section.

The concrete damage plasticity (CDP) model [20] is employed to simulate the concrete behavior due to its ability to capture the concrete crushing in compression and cracking in tension. The local crushing of the concrete may occur around the anchors while the cracking of the concrete may occur anywhere in the slab where tensile stresses are present. The Hognestad parabola [21] is used to define the stress-strain relationship of the concrete in compression (Fig. 3a), while the tension softening formulation presented in reference [20] is used to account for the post-cracking concrete resistance (Fig. 3b) due to such mechanisms as the aggregate interlock and fracture energy. The behavior of the anchor rod is modeled using the Menegotto-Pinto model (Fig. 3c) which accounts for the nonlinear strain hardening behavior after yielding. The behavior of the adhesive resin is defined according to the trilinear Eligehausen model [22] (Fig. 3d), with a linear-elastic branch, peak strength plateau, and linear post-peak softening, which represents the experimental behavior observed for most adhesive types.

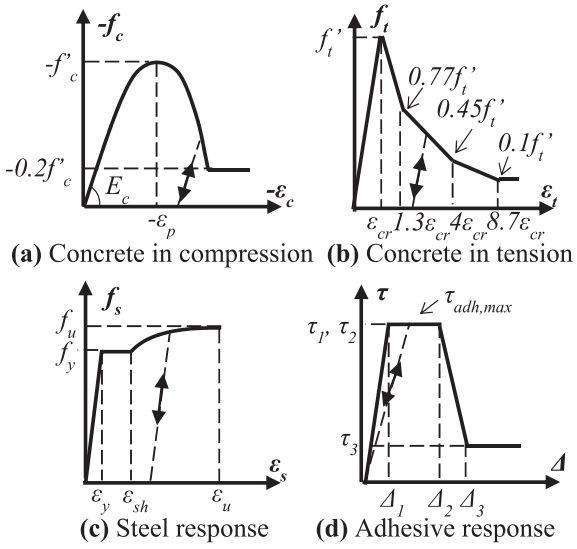

Fig. 3. Material stress-strain response models.

To validate the material models employed in the methodology, 14 3D high-fidelity NLFE models of single anchors are created and analyzed under pullout and shear loading; the simulated responses are compared with the experimental results. This validation study does not need to be repeated when applying the 2D methodology; it is conducted here to validate the material models. The experimental specimens are selected from the literature to exhibit the main types of anchor failure modes; namely steel rupture in tension, concrete breakout, bond failure, and steel fracture in shear [18]. Specimen details are presented in Table 1, where d_a is the anchor diameter, h_{ef} is the anchor embedment depth, d_{tip} is the anchor tip diameter, f'_c is the concrete compressive strength, f'_t is the concrete tensile strength, f_y is the steel yield strength, and f_u is the steel ultimate strength. More information can be found elsewhere [23–28].

During the creation of the 3D NLFE models, only one-quarter of the specimens are modeled to reduce computational demand. Eight-node 3D solid elements [29] are used when modeling the steel anchor rods and concrete regions, while cohesive elements are used when modeling the adhesive resin. A frictionless, hard contact interaction is defined to prevent interpenetration between the anchor and the concrete.

The results of the validation studies demonstrate that the proposed material models accurately capture the main anchor failure modes. In the steel rupture mode, the anchor elongates as the steel yields, reaches its ultimate strength, and ruptures near its top (Fig. 4a). In the concrete breakout mode, the concrete cracks with an angle close to 35° and comes out in a conical shape (Fig. 4b). In the bond failure mode, the anchor slides out of the borehole when the adhesive reaches its bond strength with little engagement of the concrete (Fig. 4c). In the steel failure mode in shear, bearing of the concrete occurs in the direction of the load prior to cracking and shearing of the steel anchor over its cross-section (Fig. 4d). A good agreement between the numerical and the experimental load-displacement responses is obtained in all failure modes examined albeit with an underestimation of the ductility in the shear failure mode (see the lower plots in Fig. 4a–d).

The load capacity predictions from all 14 specimens are found to be within 10% of the experimental results as shown in Fig. 5. This process validates the material models employed, and these models can be used during the creation of the 2D NLFE models without the need to repeat this validation study.

2.2. Equivalent cone Method (ECM)

The concrete thickness has a fundamental role in the concrete breakout failure mode (e.g. Fig. 4b). One limitation of 2D NLFE models is that stresses and strains are constant over the thickness of the element. However, in reality, the stresses in the concrete tend to propagate in a conical shape from the tip of the anchor towards the top of the concrete surface. When the tensile capacity of the concrete governs (i.e. concrete breakout occurs), a 3D conical cracking pattern (i.e., the concrete cone) forms, which cannot be accurately simulated by 2D NLFE models. To overcome this limitation, a modeling approach named 'the Equivalent Cone Method' is developed. The method is based on the following premises: (1) the concrete breakout manifests in a conical shape in 3D models and experiments; (2) the concrete breakout load capacity varies linearly with the thickness of the concrete in 2D NLFE models; (3) the angle of the concrete cracking can be approximately predicted by the 2D NLFE models; and, (4) the concrete breakout load capacity is proportional to the cracked surface area in the model.

The first premise is confirmed by the existing experimental observations [e.g. 23–26], the results of which are shown in Section 2.1,

Table 1
Geometric and material properties of the selected specimens.

Specimen	Failure mode	d_a mm	h_{ef} mm	d_{tip} mm	f'_c MPa	f'_t MPa	f_y MPa	f_u MPa	$\tau_{adh,max}$ MPa
D20L200W70[23]	Steel rupture in tension	17.0	200	70.0	25.0	1.65†	434	524	N/A
D20L400W70[23]	Steel rupture in tension	17.0	400	70.0	25.0	1.65†	434	524	N/A
D20L800W70[23]	Steel rupture in tension	17.0	800	70.0	25.0	1.65†	434	524	N/A
D16L160W56[23]	Steel rupture in tension	14.4	160	56.0	25.0	1.65†	434	524	N/A
D16L320W56[23]	Steel rupture in tension	14.4	320	56.0	25.0	1.65†	434	524	N/A
D20L100W70[23]	Concrete breakout	17.0	100	70.0	25.0	1.65†	434	524	N/A
D16L80W56[23]	Concrete breakout	14.4	80	56.0	25.0	1.65†	434	524	N/A
D24H150[24]	Concrete breakout	24.0	150	32.9	27.7	2.97	500*	500*	N/A
D72H450[24]	Concrete breakout	72.0	450	88.5	27.7	2.97	500*	500*	N/A
NPC440[25]	Concrete breakout	36.0	220	55.0	34.1	3.20	900	1000	N/A
Ae12[26]	Concrete breakout	12.0	60	12.0	21.8	1.54†	500*	500*	50.00*
D20H200[27]	Bond failure	20.0	200	20.0	47.8	2.28†	640	800	16.94
D12H70[28]	Bond failure	12.0	70	12.0	26.0	2.71	1080	1200	22.55
D20H200[27]	Steel fracture in shear	20.0	200	20.0	47.8	2.28†	640	800	16.94

Data source:[23–28]
† Estimated using $f_t' = 0.33\sqrt{f_c'}$ as per ACI318-19 [18].
* Estimated due to lack of data in the paper of origin.

where a conical cracking shape is observed in the specimens failing in concrete breakout. The second premise is verified by the results of six 2D NLFE analyses, which were conducted varying the concrete thickness in Specimen D24H150 from 50 to 500 mm. As a result, the load capacity is found to vary linearly with the increase in the thickness of the concrete (see Fig. 6 where R^2 is the coefficient of correlation), verifying this premise. The third and fourth premises will be verified in Section 2.2.1.

Based on these premises, the ECM calculates an equivalent concrete thickness by equating the concrete cone surface area in 3D models to the trapezoidal surface area in 2D models, as shown by the shaded areas in Fig. 7.

As per the flowchart in Fig. 8, the application of the ECM starts with the creation and analysis of a 2D NLFE model with an estimated concrete thickness equal to $3h_{ef}$. This estimation is made to be consistent with the ACI318-19 Chapter 17 recommendations [18], where the concrete cone is extended horizontally up to $1.5h_{ef}$ in all directions, resulting in an upper cone diameter equal to $3h_{ef}$. Other values of concrete thickness can also be used because the ratio of the calculated

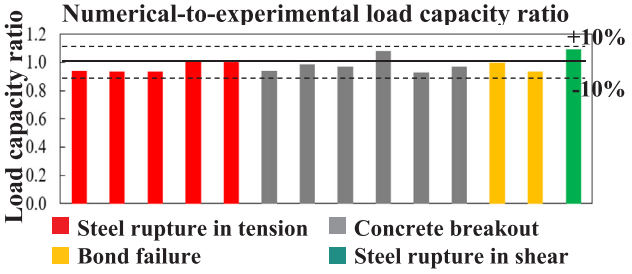

Fig. 5. 3D NLFE validation studies (14 analyses).

values will be employed when deriving t_{2D}. From this analysis, the cracking angle and vertical crack extent are extracted and used to calculate the concrete cone surface area A_{cone} (using Eq. (1)) and the trapezoidal surface area A_{trap} (using Eq. (2)). In these equations, the cracking base b_{cr} and height of the cone shape h_{cone} are taken as the anchor tip diameter and embedment depth, respectively. Eq. (3) is then used to calculate the equivalent concrete thickness t_{2D}. This concrete

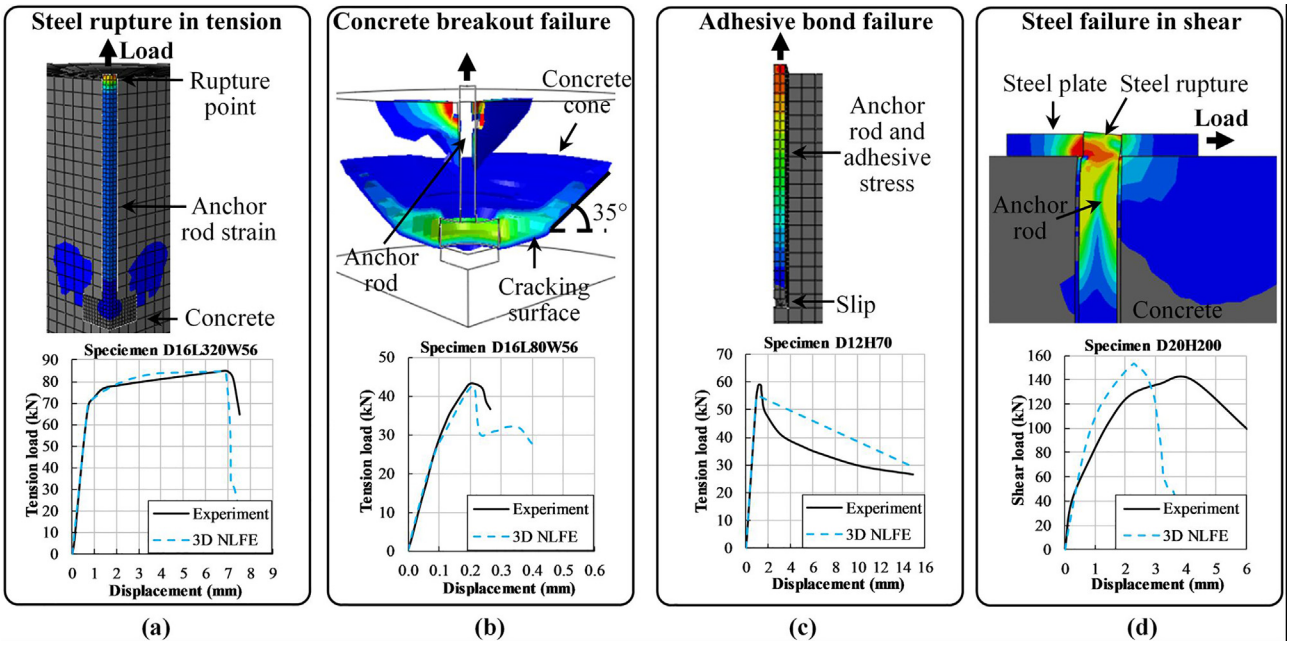

Fig. 4. Validation of the 3D NLFE models for critical failure modes.

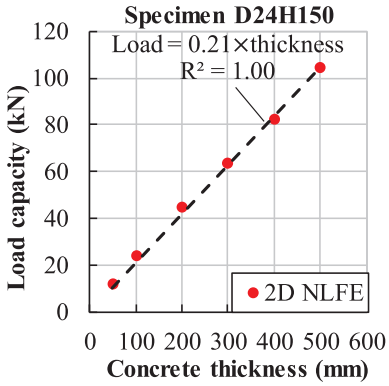

Fig. 6. Linear variation of the concrete breakout load capacity with the concrete thickness.

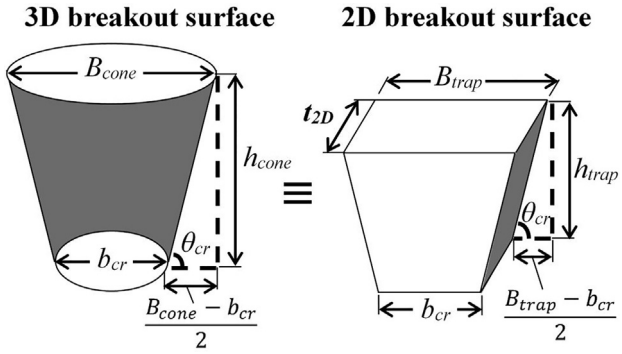

Fig. 7. Equivalent concrete breakout shapes in 3D and 2D models.

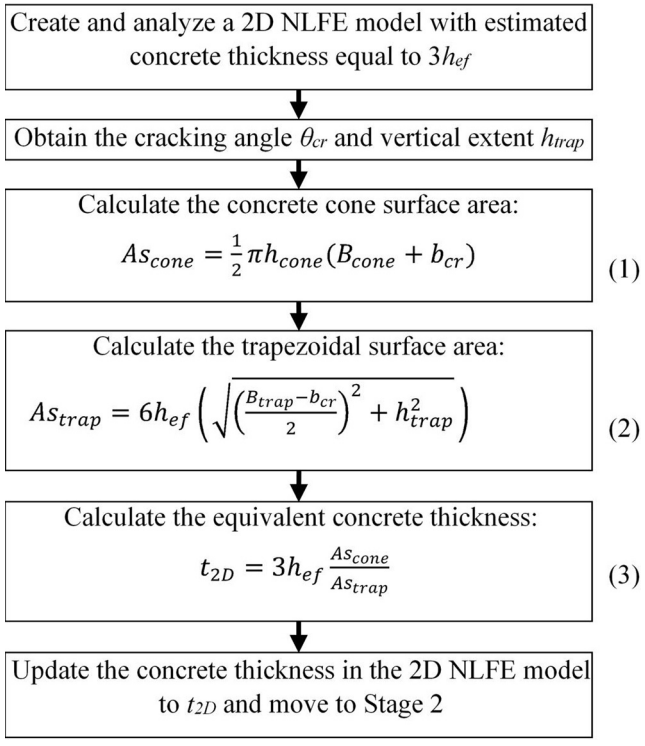

Fig. 8. Flowchart of the ECM.

thickness will be used in the creation of the actual 2D NLFE model in the second stage of the methodology. The ECM enables the 2D model to accurately predict the concrete cone capacity as equivalent to the 3D counterparts. To facilitate its application, the ECM is programmed in an

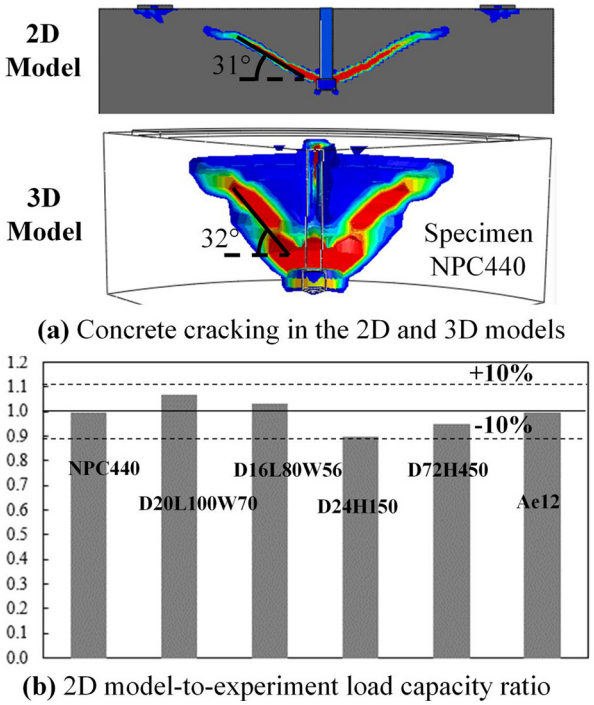

Fig. 9. Validation of the ECM.

open-access spreadsheet for the use of researchers and engineers; in addition, an educational video is created to show the proper use of the spreadsheet [30,31].

2.2.1. Validation and application of the ECM

To validate the ECM, the third and fourth premises must be verified. For this purpose, the ECM is applied to create and analyze 2D NLFE models of the six anchor specimens that exhibited concrete breakout failures. The results are compared to those from the validated 3D models and experimental tests. The cracking angles predicted by the 2D models are observed to be a good approximation of those predicted by the 3D models (see Fig. 9a for one example), which verifies with the third premise of the method. In addition, the load capacities from the 2D models agree very well with the experimental ones shown in Fig. 9b, with up to 10% of discrepancy in all cases, which verifies the fourth premise.

2.3. Wind-induced bending of NSC-supporting beams in system-level analyses

The second stage of the methodology accounts for bending of the NSC-supporting beams in system-level analyses. Current anchor analysis and design provisions [e.g. 18] are typically based on the performance of single anchors. In practice, however, steel beams (also called sleepers) are commonly used to support NSCs on concrete slabs. During strong winds, the web of these beams can bend significantly, which in turn bends the anchor rod and causes additional stresses. The proposed methodology considers this phenomenon through analytical equations developed from the results of 3D NLFE analyses of NSC-anchorage systems subjected to strong wind loads.

The system investigated consists of a box-shaped NSC (e.g., an HVAC) supported by two steel beams which are placed parallel to the wind direction and anchored to the concrete roof slab, with a compressive strength of 27.6 MPa, by four adhesive anchors at their corners as shown in Fig. 10. The design load was calculated as per reference [19] for the hurricane category 5 in the Saffir-Simpson scale (i.e., wind speed = 70 m/s). A commercially available anchor size that can safely

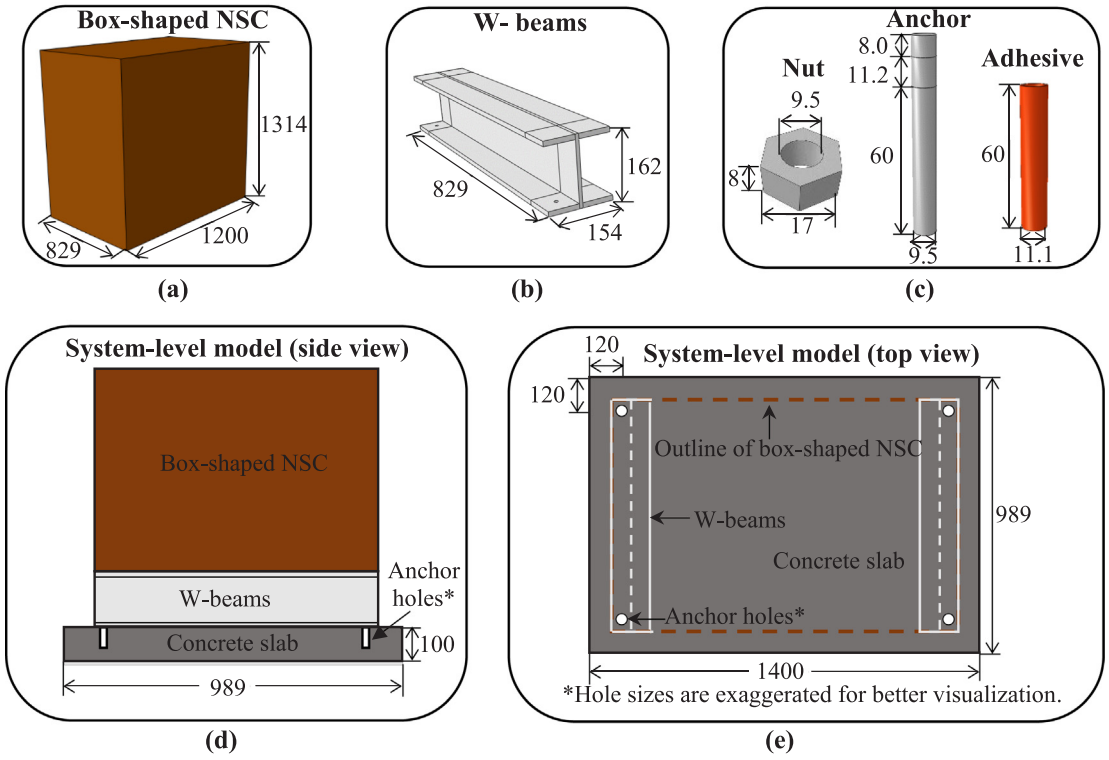

Fig. 10. NSC-anchorage system components and layout (dimensions in mm).

resist the resulting wind loads was selected as shown in Fig. 10c.

In the system-level modeling, the NSC and W beams were modeled as linear-elastic since their stress levels do not exceed the elastic range. The steel anchor, concrete, and adhesive were modeled nonlinearly according to the material models validated in Section 2.1. Full details of the system design and modeling can be found elsewhere [32].

Wind creates simultaneously applied forces, including uplift due to the suction on the top surface, lateral pressure on the leeward side, and suction on the windward side of the NSC (Fig. 11a). When applied to the system, this causes the NSC to tip in the direction of the wind (Fig. 11b) with the two anchors on the leeward side experiencing tension and the two anchors on the windward side experiencing compression. The reactions from the anchors in tension cause the beam to bend significantly perpendicular to the wind. This action, in turn, bends the top of the anchors and causes additional stresses (Fig. 11c). To quantify this phenomenon, 28 system-level NLFE analyses were performed by varying the W-beam web thickness and the distance from the center of the anchor to the center of the beam web, called “eccentricity” hereafter (Fig. 11c).

In the first seven analyses, the eccentricity distance (*ecc*) was varied from 0 to 67 mm, which is the maximum permissible for the bottom flange width of this beam, while the web thickness (t_w) was kept as 8.1 mm. Bond failures of the anchors at their full capacity (i.e., 8.4 kN) are predicted for eccentricities below 47 mm (horizontal lines in Fig. 12a) while anchor rod steel failures are predicted above this value (inclined lines in Fig. 12a). The eccentricity distance at which the failure mode changes and the load capacity reduces is termed as ‘critical eccentricity’ (ecc_{cr}), shown with red circles in Fig. 12a where the inclined lines intersect the horizontal ones. Beyond this critical eccentricity, the anchor load capacity reduces linearly with the increase in the eccentricity (Fig. 12a). This phenomenon can be explained by the linear increase in the bending moment experienced by the web when the anchor is moved away from the web of the beam, increasing the moment arm linearly. In the remaining 21 analyses, t_w was varied from 4.3 to 6.6 mm (i.e., commercially available values) for the same range of eccentricity. The critical eccentricity decreased rapidly as the web thickness was reduced, which means that when slender beams are used, the anchors should be installed closer to the web to avoid this

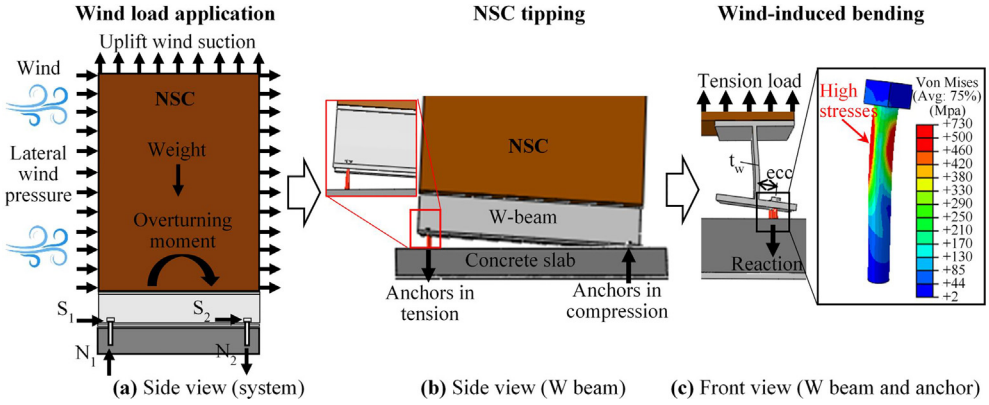

Fig. 11. System-level response including NSC tipping and wind-induced beam bending.

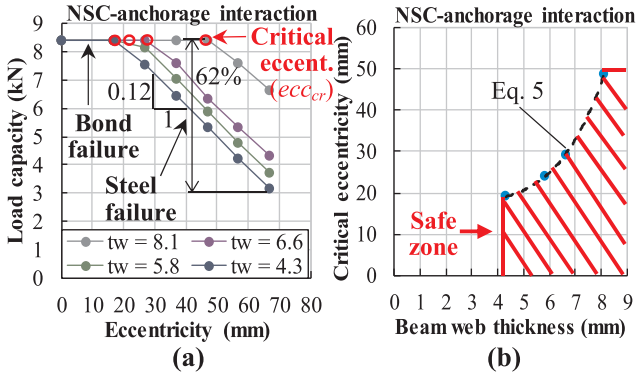

Fig. 12. (a) Influence of *ecc* and t_w on the anchor capacity, and (b) relationship between t_w and ecc_{cr}.

phenomenon. In the most severe case, a 62% decrease in the load capacity was observed.

To provide guidance on how to avoid the premature anchor rod failures due to the bending of the supporting beams, the relationship between the critical eccentricity and the beam web thickness was studied. A cubic relationship was found between these two parameters (Fig. 12b), which is attributed to the cubic variation of the web moment of inertia with its thickness. It is recommended, during the design, that the eccentricity distance and the web thickness be selected to remain below and to the right of the cubic curve, respectively, as shown in Fig. 12b as the "safe zone".

The proposed methodology considers the wind-induced bending effects by reducing the anchor rod rupture capacity (P_{red}) according to Eqs. (4) and (5), derived from the results shown in Fig. 12. This procedure permits modeling this 3D system-level phenomenon using 2D models.

$$P_{red} = \min(P_{max} - 0.12 \times (ecc - ecc_{cr}), P_{max}) \tag{4}$$

$$ecc_{cr} = 0.27t_w^3 - 3.00t_w^2 + 12.24t_w \tag{5}$$

where P_{red} is the reduced anchor load capacity in steel rupture failure mode due to the bending effects, and P_{max} is the full load capacity of the anchor in bond failure mode.

2.4. Artificial neural network to account for concrete cracking

The third stage of the methodology accounts for the detrimental effects of long-term concrete cracking, which is commonly observed on rooftop slabs. These cracks form due to the repetitive and long-term application of service loads to the roof slabs. These cracks, in the long run, create discontinuities in the bond between the adhesive resin and the surrounding concrete [17], weakening the bond prior to the incidence of windstorms. There is a scarcity of NLFE material models that can capture this phenomenon. To bridge this gap, a novel artificial neural network is developed as a part of the proposed methodology.

ANNs are a versatile mathematical tool that can 'learn' complex relationships between input and output. When 'trained' with experimental data, ANNs can predict the result instantaneously, which makes them ideal for predicting the anchor capacity in cracked concrete.

The development of an accurate ANN relies on testing and optimizing various configurations of trained ANNs; therefore, the training process will be discussed first. For training, experimental data from anchor tests was obtained from the worldwide database maintained by the ACI Committee 355, which contains experimental results from 38 papers and reports from the USA, Europe, and Japan [33]. For achieving this study's goal, 160 specimens were available since they satisfied the following requirements: (*i*) anchor installations were conducted in cracked concrete; (*ii*) boreholes were cleaned and dried; (*iii*) load was applied as static tension; and (*iv*) anchors were tested individually. The adhesive type used in all specimens was Vynilester. To provide the most applicability, it was ensured that the training and testing sets (i.e. the specimens used for the training and testing, respectively) cover the entire range of each input parameter. The training set consisted of 144 specimens (90%) and the remaining 16 specimens (10%) were used as the testing set, a rate used by other researchers [34–36]. Additional details on the selected database can be found in [32].

The ANN is trained by applying the forward and back propagation techniques repeatedly in an iterative process. During the forward propagation, each neuron in the developed ANN modifies the input (x) according to the weights (w) and biases (b) associated with each neuron as per Eq. (6) to obtain the net input (u), which is further modified by the activation function (Eq. (7)) to generate the output (y). The sigmoid is used as the activation function due to its advantageous characteristics of accepting any input in the real domain and being smooth. After the final output is calculated, the back propagation is performed by calculating the error (E) between the target load capacity (P_{Target}) and the ANN prediction (P_{ANN}) as per Eq. (8). The developed ANN uses the derivative of this error to update the weights and biases as per Eqs. (9) and (10), which makes them converge to optimum values, leading to accurate predictions after a sufficient number of iterations. A learning rate (η) of 0.5 is multiplied by the error derivative in these equations, which helps prevent overfitting and ensures that the ANN results can be generalized. To increase the convergence rate of the weights and biases, the inputs are normalized to be within 0 and 1, which is the region where the sigmoid has the highest slope. To determine the optimum number of iterations, several training processes were performed using 10,000 to 500,000 iterations. It was found that 50,000 iterations provided sufficient accuracy without overfitting or excessive training time.

$$u_j = \sum (w_{ij} y_i + b_j) \tag{6}$$

$$y_j = \frac{1}{1 + \exp(-u_j)} \tag{7}$$

$$E = \frac{1}{2} \sum (P_{ANN} - P_{Target})^2 \tag{8}$$

$$w = w - \eta \frac{\partial E}{\partial w} \tag{9}$$

$$b = b - \eta \frac{\partial E}{\partial b} \tag{10}$$

To obtain the most accurate prediction of the anchor load capacity, various ANN configurations (i.e. number of neurons, number of layers, and input variables) were created, trained, and evaluated in terms of their total error and training time; see the details in [32]. As a result, the optimum ANN configuration was determined to be the one shown in Fig. 13. In this configuration, the input layer consists of five neurons receiving the concrete compressive strength (f'_c), the anchor diameter (d_a), the anchor embedment depth (h_{ef}), the annular gap (A_g, i.e. space between the anchor and the borehole in which the adhesive is placed), and the concrete crack width (w_{cr}). The output layer (i.e. the last layer)

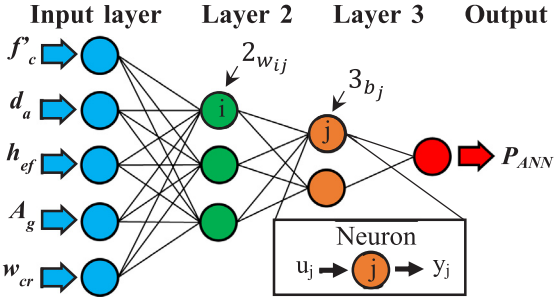

Fig. 13. ANN configuration developed.

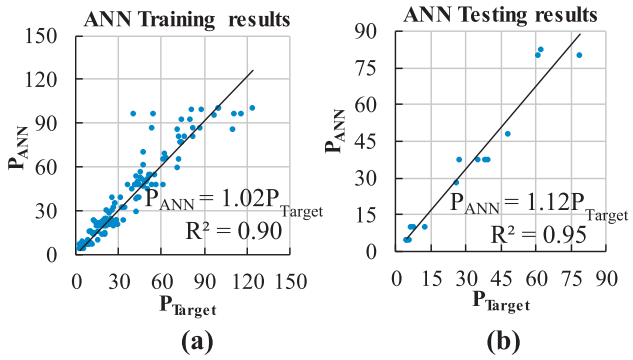

Fig. 14. Prediction accuracy of the developed ANN.

consists of one neuron that returns the predicted load capacity of the adhesive anchor (P_{ANN}).

In this configuration, the ANN training takes only 12 s (using a laptop computer with 7th Gen. Intel i5-7200 CPU, 8 GB RAM, and 1 TB hard drive) and leads to accurate predictions of the anchor load capacities which are nearly equally above and below the experimental results, presenting no clear bias (see Fig. 14a). To test the general applicability, the trained ANN was used to predict the load capacities of 16 specimens from the database that were not used during the training. The accuracy obtained in the testing is even higher than that in the training (Fig. 14b), confirming the applicability of the ANN to new specimens.

To facilitate the application of the trained ANN in its optimum configuration, an open-access spreadsheet [37] is developed, which rapidly and accurately calculates the anchor load capacities (P_{ANN}) in cracked concrete. Eq. (11) is then employed to calculate the reduced bond strength of the adhesive in cracked concrete (τ_{cr}) for use in the NLFE simulation during the definition of the adhesive material model, allowing the cracking effects to be accounted for without any additional computational cost. An educational video is also created to demonstrate the proper use of the spreadsheet [38].

$$\tau_{cr} = \frac{P_{ANN}}{\pi(d_a + 2A_g)h_{ef}} \tag{11}$$

2.5. Analytical equations for the adhesive model in elevated temperatures

The fourth stage of the methodology accounts for the bond deterioration due to elevated temperatures commonly encountered on the rooftops in hurricane-prone regions. To achieve this objective, Eqs. (12) and (13) are derived based on the experimental data from 16 anchor tests performed in reference [16] (Fig. 15a, b). These equations are applied to modify the adhesive strength (τ_{adh}) and stiffness (E_{adh}) as a function of the temperature ($Temp$), where the maximum strength ($\tau_{adh,\max}$) and stiffness ($E_{adh,\max}$) represent unreduced values at normal temperatures (e.g. lower than 40 °C). After this modification, the desired temperature is applied to the adhesive prior to the load/displacement application.

$$\tau_{adh} = \min(0.0001 \times Temp^2 - 0.0275 \times Temp + 1.9516, 1)\tau_{adh,max} \tag{12}$$

$$E_{adh} = \min(-7.2 \times 10^{-7} \times Temp^3 + 2.86 \times 10^{-4} \times Temp^2 - 0.037 \times Temp + 1.57, 1)E_{adh,max} \tag{13}$$

To demonstrate how this modification in the adhesive model affects the anchor response, Specimen D12H70 [28] is re-analyzed subjected to 38, 60, and 82 °C (100, 140, and 180 °F), representing possible rooftop temperatures [15]. The effect of these temperatures on the concrete and steel properties are negligible; therefore, they do not need to be considered. The load–displacement responses obtained indicate a

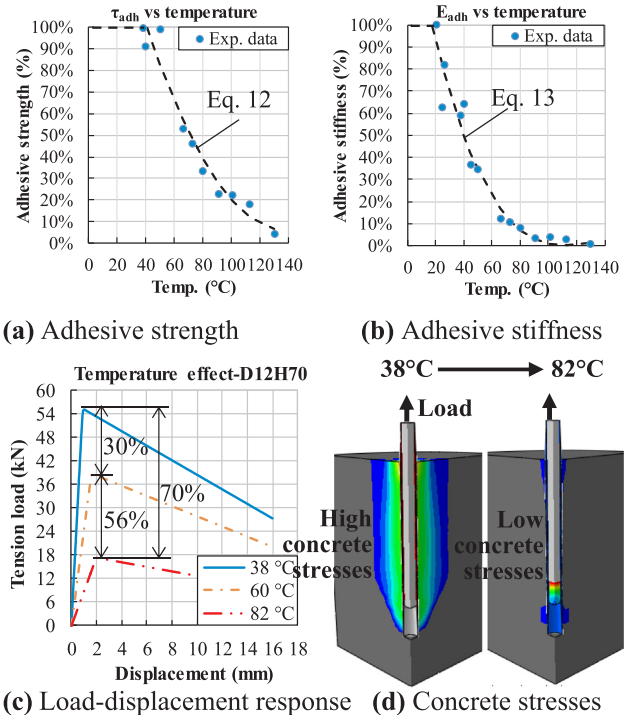

Fig. 15. Effects of elevated temperatures.

significant reduction in anchor load capacity and initial stiffness, up to 70% at 82 °C (Fig. 15c). In addition, the stresses transmitted to the surrounding concrete at failure decrease with the increase in temperature due to the reduced bond between the anchor rod and surrounding concrete (Fig. 15d).

3. Summary and conclusions

In this study, a 2D anchor analysis methodology is developed combining numerical modeling and artificial neural network (ANN) techniques to rapidly simulate both the single-anchor and system-level NSC-anchorage response while accounting for the adverse environmental exposure experienced by the rooftop slabs and the detrimental effects of wind-induced bending. The following conclusions are drawn from this study:

- The adverse environmental exposure and wind-induced bending may significantly reduce an anchor's performance and promote premature anchor failure.
- The nonlinear material models employed in the proposed 2D NLFE methodology accurately simulate the response of the concrete, steel, and adhesive as demonstrated by the 3D high-fidelity NLFE simulations.
- The Equivalent Cone Method (ECM) permits the use of 2D models to accurately simulate the 3D concrete breakout failure mode. The ECM determines an equivalent concrete thickness which permits the load capacity predictions from 2D models to match those from 3D models in concrete breakout failure mode. The open-access spreadsheet created during this study facilitates the application of the ECM.
- The 3D NSC-anchorage system analyses reveal that anchor damage due to wind-induced bending of NSC-supporting beams may cause premature anchor rod failures for eccentricity distances beyond a critical value, reducing the anchor capacity by up to 62% in this study. The equations developed calculate this critical eccentricity and reduce the anchor load capacity for use in the 2D NLFE models.
- The developed multilayered feed-forward ANN can rapidly and

accurately predict the capacities of adhesive anchors installed in cracked concrete. The open-access spreadsheet created during this study allows easy execution of the formulations of this ANN.
- The proposed methodology is capable of accounting for the effects of concrete cracking in 2D NLFE analyses by calculating a reduced bond strength using the results from the ANN.
- The two analytical equations derived enable quantifying the strength and stiffness degradation of adhesives at elevated temperatures when performing 2D NLFE analyses. The results show that the anchor load capacity is reduced significantly, by up to 70%, when the adhesive temperature is increased from 38 to 82 °C.
- The proposed 2D methodology takes a fraction of the time required by 3D models while achieving load capacity prediction accuracies similar to the 3D models and accounting for concrete cracking, elevated temperatures, concrete cone failure, and wind-induced bending effects.

Declaration of Competing Interest

None.

Acknowledgments

The authors would like to thank Dr. Ronald A. Cook for providing the worldwide database for adhesive anchors in cracked concrete and Dr. Arindam G. Chowdhury for providing the wind load data used in this study.

Appendix A. Supplementary material

Supplementary data to this article can be found online at https://doi.org/10.1016/j.engstruct.2020.110505.

References

[1] NOAA. U.S. billion-dollar weather and climate disasters. NOAA National Centers for Environmental Information (NCEI); 2019. Accessed April 26, 2019, from < https://www.ncdc.noaa.gov/billions/summary-stats > .
[2] Guo J. The costs of climate change. In: IOP Conf. Series: Earth and Environmental Science 120, 012015, Singapore; 2018. p. 7. < https://iopscience.iop.org/article/10.1088/1755-1315/120/1/012015/pdf > .
[3] Dinan T. Projected increases in hurricane damage in the United States: the role of climate change and coastal development. Ecol Econ 2017;138:186–98. https://doi.org/10.1016/j.ecolecon.2017.03.034.
[4] Cui W, Caracoglia L. Exploring hurricane wind speed along US Atlantic coast in warming climate and effects on predictions of structural damage and intervention costs. Eng Struct 2016;122:209–25. https://doi.org/10.1016/j.engstruct.2016.05.003.
[5] Liu F. Projections of future US design wind speeds due to climate change for estimating hurricane losses. Ph.D. Thesis. Clemson University, South Carolina, U.S.A.; 2014. p. 256 < https://tigerprints.clemson.edu/all_dissertations/1305 > .
[6] Michalski J. Building exposure study in the state of Florida and application to the Florida public hurricane loss model. M.S. Thesis. Florida Institute of Technology, Florida, U.S.A.; 2014. p. 166 < http://hdl.handle.net/11141/1074 > .
[7] Mudd L, Wang Y, Letchford C, Rosowsky D. Assessing climate change impact on the U.S. east coast hurricane hazard: temperature, frequency and track. Nat Hazard Rev 2014;04014001. https://doi.org/10.1061/(ASCE)NH.1527-6996.0000128.
[8] Emanuel KA. Downscaling CMIP5 climate models shows increased tropical cyclone activity over the 21st century. PNAS 2013;110(30):12219–24. https://doi.org/10.1073/pnas.1301293110.
[9] Knutson TR, Sirutis JJ, Vecchi GA, Garner S, Zhao M, Kim H-S, et al. Dynamical downscaling projections of twenty-first-century Atlantic hurricane activity: CMIP3 and CMIP5 model-based scenarios. Am Meteorol Soc 2013;26:6591–617. https://doi.org/10.1175/JCLI-D-12-00539.1.
[10] Cope AD. "Predicting the vulnerability of typical residential buildings to hurricane damage". Ph.D. Thesis. Florida, U.S.A: University of Florida; 2004. p. 222 pp..
[11] Sun Light & Power. Solar power systems have benefitted the multifamily industry for decades. Sun Light & Power; 2018. Accessed October 05, 2019, from < https://sunlightandpower.com/portfolio/multifamily-affordable-housing-solar/ > .
[12] Cappucci M, Samenow J. Bomb cyclone bolts toward upper Midwest after blasting Colorado and the Plains. The Washington Post. Accessed October 05, 2019 from < https://www.washingtonpost.com/weather/2019/03/14/bomb-cyclone-bolts-toward-upper-midwest-after-blasting-colorado-plains/ > .
[13] Simon J. A lonely aerial view of Irma's destruction in Florida Keys Accessed October 05, 2019, from < https://qz.com/1078828/hurricane-irma-damage-an-aerial-view-of-the-destruction-irma-left-behind-in-the-florida-keys/ > QUARTZ; 2017.
[14] U.S. Department of Homeland Security; 2018. Attachment of rooftop equipment in high-wind regions. FEMA, 8 pp.
[15] Winandy JE, Wolde AT, Falk RH, Barnes HM. Temperature histories of plywood roof sheathing and roof rafters as used in North America light-framed construction. In: Proceedings of the 7th World Conference on Timber Engineering, Shah Alam, Malaysia; 2002. p. 114–21. < https://www.fpl.fs.fed.us/documnts/pdf2002/winan02b.pdf?fbclid=IwAR0MssjbOIAraFaP90Kt5q9BvzQvRisTL9jRe6jy0t4HheCn1d8nrelX9d0 > .
[16] Lahouar MA, Caron J-F, Pinoteau N, Forêt G, Benzarti K. Mechanical behavior of adhesive anchors under high temperature exposure: experimental investigation. Int J Adhes Adhes 2017;78:200–11. https://doi.org/10.1016/j.ijadhadh.2017.07.004.
[17] Eligehausen R, Balogh T. Behavior of fasteners loaded in tension in cracked reinforced concrete. ACI Struct J 1995;92–S35:365–79. < https://www.concrete.org/publications/internationalconcreteabstractsportal/m/details/id/1137 > .
[18] ACI Committee 318. Building code requirements for structural concrete (ACI 318-19) and commentary. American Concrete Institute, Farmington Hills, MI; 2019. p. 519 < https://www.concrete.org/tools/318buildingcodeportal.aspx.aspx > .
[19] American Society of Civil Engineers (ASCE). Minimum design loads and associated criteria for buildings and other structures (ASCE/SEI 7-16). American Society of Civil Engineers, Reston, VA; 2016. p. 822 < https://www.asce.org/asce-7/ > .
[20] Wahalathantri BL, Thambiratnam DP, Chan THT, Fawzia S. A material model for flexural crack simulation in reinforced concrete elements using Abaqus. In: Proceedings of the first international conference on engineering, designing and developing the built environment for sustainable wellbeing, Brisbane, Australia; 2011. p. 260–4.
[21] Sagbas G. Nonlinear finite element analysis of beam-column subassemblies. M.S. Thesis. University of Toronto, Ontario, Canada; 2007. p. 182 < http://vectoranalysisgroup.com/theses/Sagbas-MASc(2007).pdf > .
[22] Eligehausen R, Popov EP, Bertéreo VV. Local bond-stress relationship of deformed bars under generalized excitations. Proceedings of the 7th European Conference on Earthquake Engineering, Athens, Greece. 1982. p. 69–80.
[23] Tsavdaridis KD, Shaheen MA, Baniotopoulos C, Salem E. Analytical approach of anchor rod stiffness and steel base plate calculation under tension. Structures 2016;5:207–18. https://doi.org/10.1016/j.istruc.2015.11.001.
[24] Eligehausen R, Bouska P, Cervenka V, Pukl R. Size effect of the concrete cone failure load of anchor bolts. Invited paper; 1992. p. 517–25. < http://elib.uni-stuttgart.de/handle/11682/7911 > .
[25] Nilforoush R, Nilsson M, Elfgren L. Experimental evaluation of tensile behaviour of single cast-in-place anchor bolts in plain and steel fibre-reinforced normal- and high-strength concrete. Eng Struct 2017;147:195–206. https://doi.org/10.1016/j.engstruct.2017.05.062.
[26] Hoehler MS, Mahrenholtz P, Eligehausen R. Behavior of anchors in concrete at seismic-relevant loading rates. ACI Struct J 2011;108–S24:238–47.
[27] Epackachi S, Esmaili O, Mirghaderi SR, Behbahani AAT. Behavior of adhesive bonded anchors under tension and shear loads. J Constr Steel Res 2015;114:269–80. < http://dx.doi.org/10.1016/j.jcsr.2015.07.022 > .
[28] Marcon M, Vorel J, Nincević K, Wan-Wendner R. Modeling adhesive anchors in a discrete element framework. Materials 2017;10917: 1–23. < https://www.researchgate.net/publication/318993125_Modeling_Adhesive_Anchors_in_a_Discrete_Element_Framework > .
[29] ABAQUS 6.14. Analysis user's guide Vol. IV, Dassault Systems, Providence, Rhode Island; 2014. p. 1098.
[30] Almeida Jr SA, Guner S. Equivalent Cone Method (ECM), Excel Spreadsheet, University of Toledo; 2019a. < http://www.utoledo.edu/engineering/faculty/serhan-guner/docs/5S_Equivalent_Cone_Method_ECM.xlsx > .
[31] Almeida Jr SA, Guner S. Equivalent cone method (ECM)", Video, University of Toledo; 2019b. < https://www.youtube.com/watch?v=I3lpxFPtduM&feature=youtu.be > .
[32] Almeida Jr, SA. Modeling of concrete anchors supporting non-structural components subjected to strong wind and adverse environmental conditions." M.S. Thesis. University of Toledo, Ohio, U.S.; 2019. 90 p. < http://www.utoledo.edu/engineering/faculty/serhan-guner/docs/T6_Almeida_MS_2019.pdf > .
[33] Sakla SSS, Ashour AF. Prediction of tensile capacity of single adhesive anchors using neural networks. Comput Struct 2005;83:1792–1803. 10.1016/j.compstruc.2005.02.008.
[34] Gesoglu M, Güneyisi EM, Güneyisi E, Yilmaz ME. Mermerdas K. Modeling and analysis of the shear capacity of adhesive anchors post-installed into uncracked concrete. Composites: Part B 2014;60: 716–724. < http://dx.doi.org/10.1016/j.compositesb.2014.01.015 > .
[35] Gesoglu M, Güneyisi E. Prediction of load-carrying capacity of adhesive anchors by soft computing techniques. Mater Struct 2007;40: 939–951. < https://doi.org/10.1617/s11527-007-9265-6 > .
[36] Ashour AF, Alqedra MA. Prediction of shear capacity of single anchors located near a concrete edge using neural networks. Comput Struct 2005;83: 2495–2502. 10.1016/j.compstruc.2005.03.019.
[37] Almeida Jr SA, Guner S. "Artificial neural network for adhesive anchors in cracked concrete", Excel Spreadsheet. University of Toledo. 2019. < http://www.utoledo.edu/engineering/faculty/serhan-guner/docs/4S_ANN_Adhesive_Anchors_Cracked_Concrete.xlsx > .
[38] Almeida Jr SA, Guner S. "Artificial neural network for adhesive anchors in cracked concrete", Video. University of Toledo 2019. < https://www.youtube.com/watch?v=6mAQPRJDQKM&feature=youtu.be > .